Supplementary Material (ESI) for *Soft Matter*

Supplementary Information

Tunable Supramolecular Networks via *Cis-Trans* Metal-Ligand Isomerization

Shihu Wang and Elena E. Dormidontova*

*Department of Macromolecular Science and Engineering, Case Western Reserve University, Cleveland, Ohio 44106. *E-mail: eed@case.edu*

Angle distribution and energy consideration

As shown in Figure 1 in the main text, for *cis*- and *trans*- isomers there are different preferable angles between ligands in 2:1 ligand-metal complexes: θ_0=120° and θ_0=180° respectively[1]; while in 3:1 ligand-metal complexes ligands are homogeneously distributed around the metal with an average angle between any two ligands θ_0=120°. In our Monte Carlo simulations a reversible coordination bond between a metal and a ligand is formed during a bonding update with a probability proportional to exp(-$\Delta F/k$T) where $\Delta F=\Delta E+T\Sigma\Delta S$ includes both the enthalpic gain for bond formation and the entropic penalty for bond orientation. The latter has the following form:

$$\Delta S = B\left(1-\cos\left(\theta-\theta_0\right)\right) \quad (1)$$

where θ is the angle between the tangential directions of two neighboring coordination bonds belonging to the same metal and B (in units of Boltzmann constant k) characterizes the orientational penalty for deviation from the preferable angle (θ_0). By varying parameter B, different angle distributions for *cis*- and *trans*- isomers can be obtained. Firstly, the angle distribution around each preferable angle was determined by averaging simulation data over

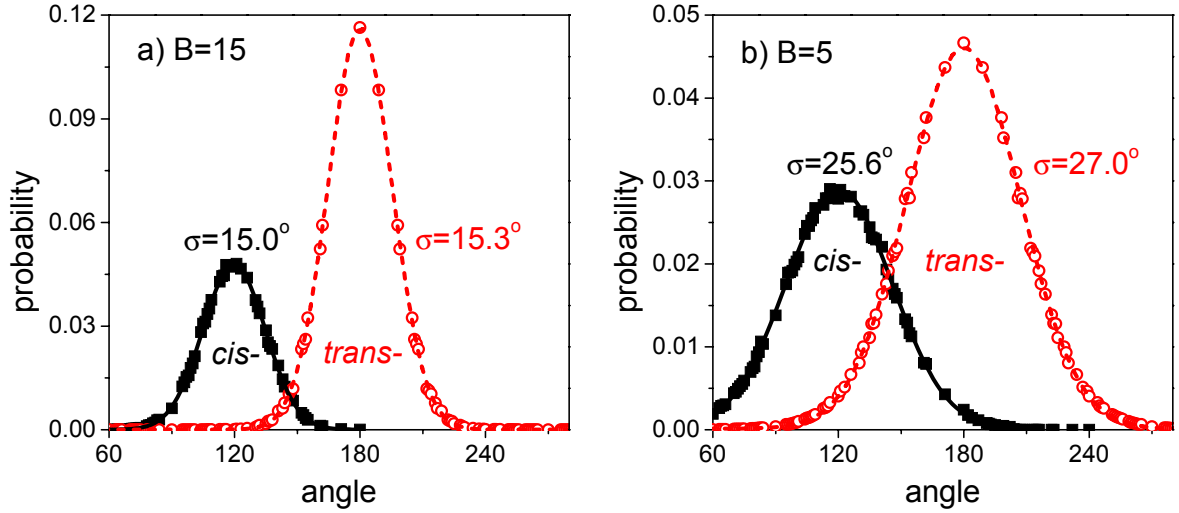

Fig. S1 Angle distribution for the *cis*- (filled symbols) and *trans*- (open symbols) 2:1 ligand-metal complexes obtained from normalized simulation data (see text) for oligomer number density c=3.8×10^{-4} a^{-3} at the stoichiometric composition for the rigidity parameter B=15 (a) and B=5 (b). The curves are a fit to a Gaussian function.

4×10^6 Monte Carlo timesteps (MCts). Additionally we need to take into account that in the bond fluctuation model (BFM)[2, 3] each monomer has 108 neighbors on the cubic lattice, and therefore only a range of particular angles (between the coordination bonds belonging to the same metal) are available (with angle 90° having the largest probability to occur). Thus to obtain the average angle distribution for each isomer we normalized the corresponding simulation data by the occurrence probability of each angle in BFM.

The average angle distributions for *cis*- and *trans*- 2:1 ligand-metal complexes are shown in Figure S1a for B=15. As is seen each distribution follows a Gaussian function with expected average values of θ=120.0° for *cis*- isomers and θ=180.0° for *trans*-isomers and variances σ=15.0° and σ=15.3°, respectively. Smaller B values provide considerably wider overlaping distributions between *cis*- and *trans*- isomers making difficult any distinction between these two cases (Figure S1b). On the other hand much larger B values lead to more

narrow distributions limiting the occurrence of 2:1 ligand-metal complexes. It is worthwhile to note that the peak heights of the angle distributions for *cis*- and *trans*- isomers are different because of the different number of discrete angles (shown as symbols in Figure S1) that contribute to the distribution.

For the 3:1 ligand-metal complexes, which are similar for both *cis*- and *trans*- isomers, B=5 was chosen, which resulted in a Gaussian distribution (not shown) with a mean value of θ=120.0° and variance σ=24.1°. We note that formation of 3:1 ligand-metal complexes involves a considerable orientation limitation for the positioning of the ligands involved, which implies that the strength of orientational penalty, B, cannot be too large for the corresponding complexes to form. It is important to note that all angle distributions discussed above are independent of oligomer number density and metal-to-oligomer ratio.

Having set B values related to the entropic penalty and orientational distributions for 2:1 and 3:1 ligand-metal complexes for *cis*- and *trans*- isomers, the association energies ΔE_i for the formation of the first (i=1), second (i=2) and third (i=3) coordination bond between a metal and ligands were chosen to represent the equilibrium constants for *cis*-complexation between Co^{2+} and 2,2'-bipyridyl[4] ($LogK_1$=5.81, $LogK_2$=5.5, $LogK_3$=4.87). As discussed in the main text the equilibrium constants are connected with the association energies and the fraction of metal-ligand complexes via eq 2. Specifically, K_i were calculated from simulation data using $K_1 = \frac{[LM]}{[L][M]}$, $K_2 = \frac{[L_2M]}{[L][LM]}$, $K_3 = \frac{[L_3M]}{[L][L_2M]}$ (cf. eq 2), where [L], [M], [LM], [L_2M] and [L_3M] is the number density of free ligands, metal ions, 1:1, 2:1 and 3:1 ligand-metal complexes, respectively. By varying ΔE_i in our simulations and comparing the equilibrium constants obtained from simulations and the experimental data for *cis*-complexation between Co^{2+} and 2,2'-bipyridyl[4], we determined the association energies

ΔE_1=-8kT, ΔE_2=-10kT, and ΔE_3=-10kT with the corresponding equilibrium constants $LogK_1$=5.9, $LogK_2$=5.7 and $LogK_3$=5.0. As is seen, with the chosen association energies equilibrium constants for *cis*-isomers obtained in our simulations reproduce the experimental data quite well. For *trans*-isomer, we applied the same association energies ΔE_i assuming that similar to simple ligand case[5] the enthalpic contributions to the corresponding equilibrium constants are comparable, while the main physico-chemical difference in the properties of *cis*- and *trans*- metal-ligand complexes comes from the ligand orientation.

Molecular weight distribution

The weight fraction molecular weight distributions for supramolecular polymers containing *cis*- or *trans*- isomers are shown in Figure S2 for several oligomer number densities at the stoichiometric composition r=2/3 . At low oligomer number density both types of supramolecular polymers exhibit rather similar profiles of molecular weight distribution with a slightly broader distribution for *cis*-isomer-containing polymers. In this range of number densities the weight fraction w_i of the molecules with a molecular weight of M_i decreases exponentially with molecular weight: $w_i \sim \exp(-\lambda M_i)$ with λ being the decay constant. With an increase of oligomer number density the weight fraction molecular weight distribution starts firstly to develop a plateau and then a maximum, which indicates the formation of reversible network.[6-8] The development of a plateau occurs at lower oligomer number density for supramolecular polymers containing *cis*-isomers (due to a larger fraction of *cis*-2:1 ligand-metal complexes). As is seen from Figure S2 the position of the maximum of molecular weight distribution corresponds to higher molecular weights and the peak itself is higher and narrower for supramolecular polymers containing *cis*-isomers. As oligomer number density further increases the maximum of the molecular weight distribution shifts to higher molecular weights and the Gaussian-like peak becomes even higher and narrower.

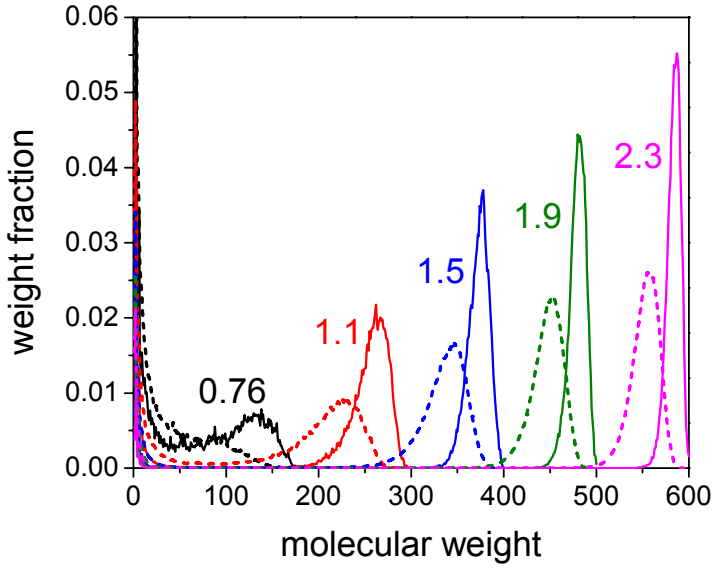

Fig. S2 Weight average molecular weight distributions for supramolecular polymers containing *cis*- (solid curves) or *trans*- (dashed curves) isomers for several oligomer number densities (shown in the units of $10^{-3}a^{-3}$) at the stoichiometric metal-to-oligomer ratio (r=0.67). Molecular weight is shown in units of oligomer molecular weight.

Since the peak development indicates network formation,[6-8] the difference in the molecular weight distributions between supramolecular polymers containing *cis*- and *trans*- isomers indicates that the formation and properties of the network are somewhat different for these polymers, as discussed in the main text.

Equilibrium elastic plateau modulus

The equilibrium high-frequency elastic plateau modulus G_0 characterizes the elastic response of the metallo-supramolecular networks to external deformation. The composition dependence of G_0 is shown in Figure S3a for two oligomer number densities. As is seen, for a given oligomer number density, the high frequency elastic plateau modulus for the reversible

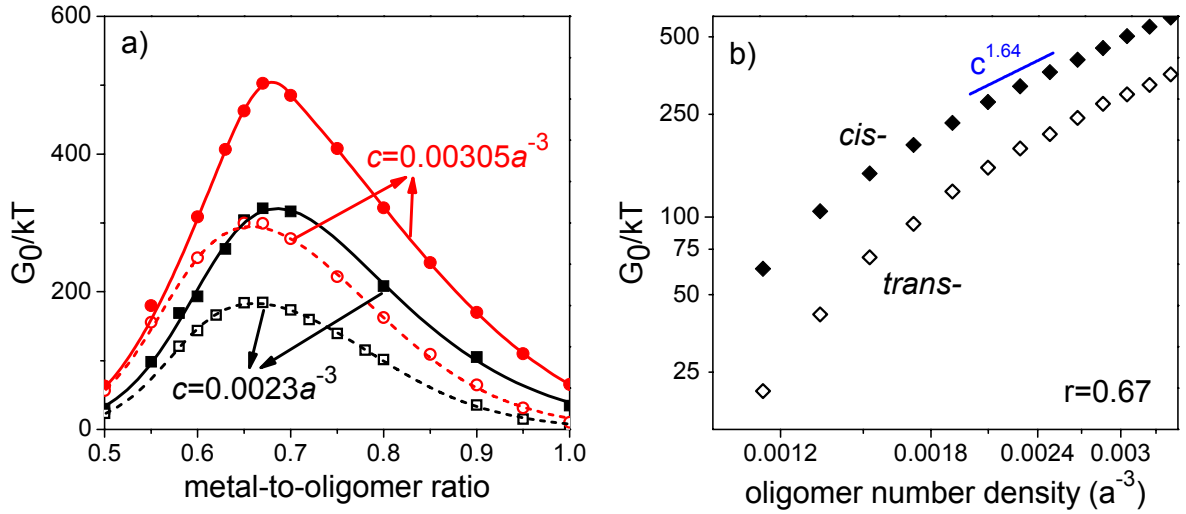

Fig. S3 The high-frequency elastic plateau modulus G_0/kT as a function of metal-to-oligomer ratio (a) at two oligomer number densities c=0.0023a^{-3} (squares) and c=0.00305a^{-3} (circles) and as a function of oligomer number density (b) at the stoichiometric composition for the reversible networks containing *cis*- (filled symbols) or *trans*- (open symbols) isomers. At high oligomer number density *cis*-isomer network is noticeably larger than that for the network containing *trans*-isomers. This is mainly because of the larger network core fraction. As is seen from Figure S3a the elastic plateau modulus G_0 exhibits a maximum around the stoichiometric composition for both networks containing *cis*- and *trans*- isomers.

For a constant metal-to-oligomer ratio, the equilibrium high-frequency elastic plateau modulus G_0 is larger for the reversible networks containing *cis*-isomers in the whole range of oligomer number densities considered. G_0 increases with an increase of oligomer number density, as shown in Figure S3b following a similar scaling dependence $G_0 \sim c^{1.64}$ at high oligomer number densities for both *cis*- and *trans*- isomer networks. The scaling factor 1.64 is rather close to what we reported before for metallo-supramolecular networks containing lanthanide metal ions (1.8)[8] or what was experimentally observed (1.8) for supramolecular

network formed by neodymium(III)-2,6-dicarboxy-pyridine ligands[9] and branched worm-like CTAB micelles, 1.85, (in the presence of salt concentration of 1.5M)[10].

Based on the results for the elastic plateau modulus presented in Figure S3, we predict that a significant change in the elastic properties of the reversible network can be achieved by an externally triggered isomerization from *trans*- to *cis*- metal-ligand complexes and vice versa.

Molecular weight between effective crosslinks

As discussed in the main text (eq 4) the average molecular weight between effective crosslinks M_e can be calculated (in addition to the direct measurements from simulations) knowing the fraction of 2:1 ligand-metal complexes in the core, M_2^{core}, and the number of effective crosslinks N_x:

$$M_e = 1 + \frac{2M_2^{core}}{3N_x} \qquad (2)$$

We note that M_2^{core} also includes 3:1 ligand-metal complexes in the core that serve as attaching points of the dangling parts, since these 3:1 ligand-metal complexes merely extend the effective strands in the core and thus perform exactly the same function as 2:1 ligand-metal complexes.

In order to compare the average molecular weight between effective crosslinks for the networks containing *cis*- (M_e^{cis}) or *trans*- isomers (M_e^{trans}) one can consider the following inequalities:

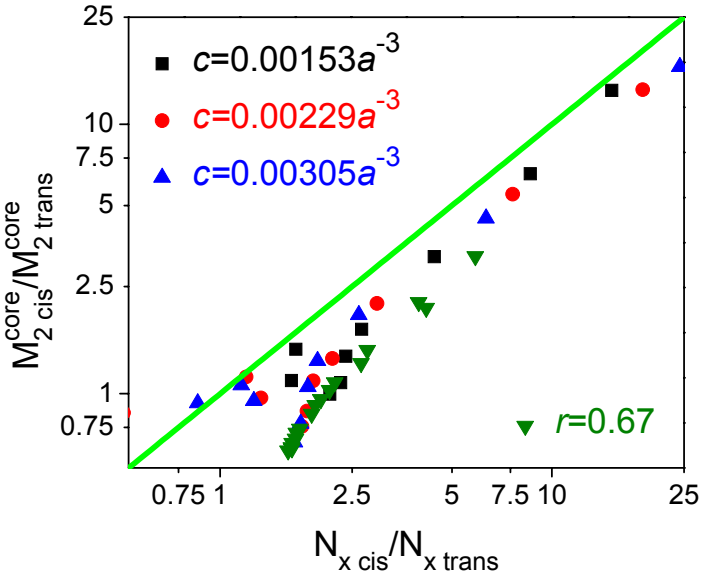

Fig. S4 $M_{2\,cis}^{core} / M_{2\,trans}^{core}$ as a function of the ratio of the effective crosslinks $N_{x\,cis} / N_{x\,trans}$ in the reversible networks containing *cis*- or *trans*- isomers. The results (symbols) are shown for several oligomer number densities (with metal-to-oligomer ratios varied) and for r=0.67 (with the oligomer number densities varied). The solid line corresponds to $M_{2\,cis}^{core} / M_{2\,trans}^{core} = N_{x\,cis} / N_{x\,trans}$.

$$M_e^{cis} = 1 + \frac{2M_{2\,cis}^{core}}{3N_{x\,cis}} < 1 + \frac{2M_{2\,trans}^{core}}{3N_{x\,trans}} = M_e^{trans} \text{ if } \frac{M_{2\,cis}^{core}}{M_{2\,trans}^{core}} < \frac{N_{x\,cis}}{N_{x\,trans}}$$

In Figure S4, we plot the ratio of $M_{2\,cis}^{core} / M_{2\,trans}^{core}$ versus the ratio of $N_{x\,cis} / N_{x\,trans}$ for the reversible networks composed of *cis*- or *trans*- isomers for several oligomer number densities and metal-to-oligomer ratios. As is seen, in all cases $M_{2\,cis}^{core} / M_{2\,trans}^{core} < N_{x\,cis} / N_{x\,trans}$, implying that M_e^{cis} is smaller than M_e^{trans}, as discussed in the main text.

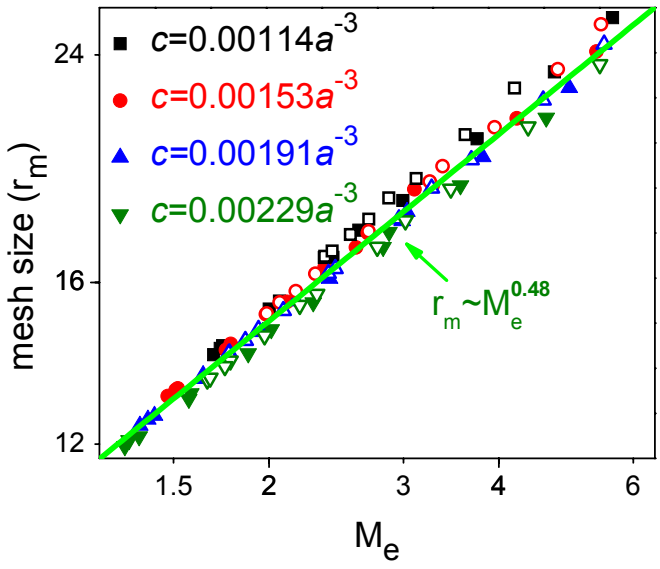

Fig. S5 The average mesh size r_m for the reversible network containing *cis*- (filled symbols) or *trans*- (open symbols) isomers versus the average molecular weight between effective crosslinks M_e for

Mesh size

Mesh size r_m is the average distance between two adjacent effective crosslinks. It was calculated by averaging over 4×10^6 MCts the end-to-end distance (R_{end}) for the effective strands connecting two neighboring effective crosslinks. The mesh size for the reversible networks containing *cis*- and *trans*- isomers r_m is plotted (in a log-log scale) in Figure S5 for different oligomer number densities (and different metal-to-oligomer ratios) versus the average molecular weight between effective crosslinks (M_e). r_m is generally larger for the reversible networks containing trans-isomers (similar to the average molecular weight between effective crosslinks, as discussed in the main text, Figure 7). The mesh size for the reversible network containing either *cis*- or *trans*- isomers follows almost the same scaling dependence: $r_m \sim M_e^{0.48}$ (for network with *trans*-isomers: $r_m \sim M_e^{0.49}$ and for network with *cis*-

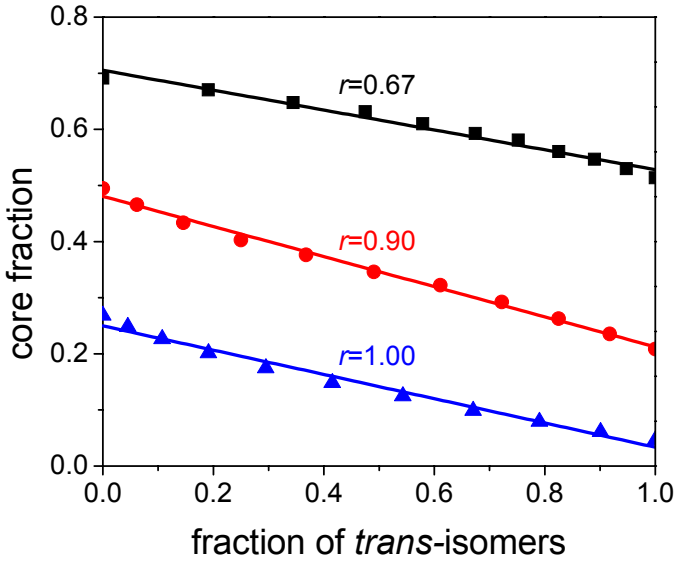

Fig. S6 Dependence of the weight fraction of the network core on the fraction of *trans*-isomers in the network at different metal-to-oligomer ratios for oligomer number density $c=2.29\times10^{-3}a^{-3}$.

isomers $r_m \sim M_e^{0.47}$). This implies that the isomerization only slightly affects the chain conformations in the core of the reversible network. This scaling dependence is similar to what we previously reported for metallo-supramolecular networks containing lanthanide metal ions ($r_m \sim M_e^{0.475}$)[8] and it is close to that for the end-to-end distance for a linear chain of a molecular weight M in a polymer melt ($R_{end} \sim M^{0.5}$). As we discussed in our earlier paper[8], the observed dependence is likely due to the high polymer density in the network core.

Mixture of *cis*- and *trans*- isomers: network core fraction

The core of the reversible network contains the effective crosslinks and elastic strands, which define the elastic properties of the metallo-supramolecular network. The weight fraction of the network core is shown in Figure S6 as a function of the fraction of *trans*-isomers f_{trans} in the system at different metal-to-oligomer ratios for oligomer number density

c=2.29×10^{-3}(a^{-3}). As is seen, the core fraction decreases in a linear manner with an increase in f_{trans} for all the metal-to-oligomer ratios considered. The maximum value of the weight fraction of the core is reached at the stoichiometric composition (similar to the elastic plateau modulus, Figures 6 and Figure S3).

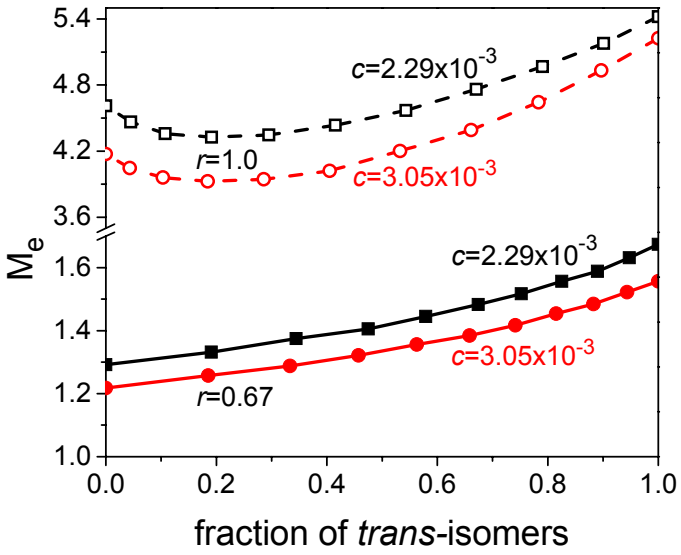

Fig. S7 The average molecular weight between effective crosslinks (M_e) as a function of *trans*-isomers fraction in the network at metal-to-oligomer ratios r=0.67 (solid symbols) and r=1.0 (open symbols) for oligomer number densities c=2.29×10^{-3} a^{-3} and c=3.05×10^{-3} a^{-3}.

Mixture of *cis*- and *trans*- isomers: average molecular weight between effective crosslinks (M_e)

Figure S7 shows the dependence of the average molecular weight between effective crosslinks (M_e) on the fraction of *trans*-isomers. As is seen, for the stoichiometric composition, the average molecular weight between effective crosslinks (M_e) is rather small and increases nearly linearly with an increase in the fraction of *trans*-isomers. For metal-to-

oligomer ratio equal to 1.0, the average molecular weight between effective crosslinks decreases at a low degree of conversion of *cis*- to *trans*- isomers and reaches its minimum at an intermediate value of f_{trans} and then increases with further increase of f_{trans}. It is interesting to note that the minimum value of M_e is smaller than in either system containing only *cis*- or only *trans*- isomers. The difference in the behaviour of the M_e at different metal-to-oligomer ratios is due to the different morphologies of networks as discussed in the main text.

References

1. Nazeeruddin, M. K.; Zakeeruddin, S. M.; Humphry-Baker, R.; Gorelsky, S. I.; Lever, A. B. P.; Gratzel, M. Coord. Chem. Rev. 2000, 208, 213 - 225.
2. Carmesin, I.; Kremer, K. Macromolecules 1988, 21, 2819 - 2823.
3. Deutsch, H. P.; Binder, K. J. Chem. Phys. 1991, 94, 2294 - 2304.
4. Smith, R. M.; Martell, A. E. Critical Stability Constants; volume 2: Amines Plenum Press: New York and London, 1975.
5. Marynick, D. S.; Askari, S.; Nickerson, D. F. Inorg. Chem. 1985, 24, 868 - 870.
6. Ballone, P.; Jones, R. O. J. Chem. Phys. 2002, 117, 6841 - 6851.
7. Baljon, A. R. C.; D., F.; Krawzsenek, D. J. Chem. Phys. 2007, 126, 044907.
8. Wang, S.; Chen, C.-C.; Dormidontova, E. E. Soft Matter 2008, 4, 2039 - 2053.
9. Vermonden, T.; van Steenbergen, M. J.; Besseling, N. A. M.; Marcelis, A. T. M.; Hennink, W. E.; Sudholter, E. J. R.; Stuart, M. A. C. J. Am. Chem. Soc. 2004, 126, 15802 - 15808.
10. Khatory, A.; Lequeux, F.; Kern, F.; Candau, S. J. Langmuir 1993, 9, 1456 - 1464.